The Journal of Neuroscience, September 1995, 15(9): 6260–6270

Anticipatory Head Direction Signals in Anterior Thalamus: Evidence for a Thalamocortical Circuit That Integrates Angular Head Motion to Compute Head Direction

Hugh T. Blair and Patricia E. Sharp

Department of Psychology, Yale University, New Haven, Connecticut 06520-8205

Several regions in the rat brain contain neurons known as head-direction cells, which fire only when the rat's head is facing in a specific direction. Head-direction cells are influenced only by the direction of the head with respect to the static environmental surroundings, and not by the position of the head relative to the body. Each head-direction cell has its own preferred direction of firing, so that together, the population of cells provides a continuous signal of momentary directional heading.

Here, head-direction cells were recorded from the postsubicular cortex (PSC) and anterodorsal nucleus (ADN) of the thalamus of freely moving rats. Cell activity was analyzed in relation to both momentary head direction, and the angular velocity of head turns. Head-direction cells in PSC maintained the same directional firing preference, regardless of the angular head velocity. By contrast, head-direction cells in ADN systematically shifted their directional firing preference, as a function of angular head velocity. The ADN cells always shifted their directional tuning peak to the left during clockwise head turns, and to the right during counterclockwise head turns. These results suggest that ADN neurons anticipate the future direction of the head, whereas PSC neurons encode the present direction of the head.

Based on these findings, we hypothesize that neurons in PSC and ADN are reciprocally connected to form a thalamocortical circuit, which computes the directional position of the rat's head by integrating the angular motion of the head over time.

[Key words: postsubiculum, anterior thalamus, head-direction cells, angular velocity, velocity integration, navigation, hippocampal formation, vestibular signals, thalamocortical loop]

The postsubicular region of the rat hippocampal formation contains neurons known as head-direction cells, which signal the direction of the animal's head in the horizontal plane (Ranck, 1984; Taube et al., 1990a,b). Each head-direction cell behaves like a neural compass, firing action potentials only when the animal's head is facing in a particular direction with respect to the static surrounding environment, regardless of the animal's location within that environment. Head-direction cells are not influenced by the position of the head relative to the body. Each cell has its own directional preference, so that together, the population of head-direction cells provides a continuous indication of the animal's directional heading.

Since the initial discovery of these cells in the postsubicular cortex (PSC), similar directional cells have been observed in several other areas, including the anterodorsal nucleus (ADN) of the anterior thalamus (Taube, 1995), the laterodorsal thalamic nucleus (LDN) (Mizumori and Williams, 1993), the retrosplenial and parietal cortical areas (Chen et al., 1990; McNaughton et al., 1991), and striatum (Wiener, 1993).

One simple explanation for the behavior of head-direction cells is that they might be driven by geomagnetic cues. However, it is possible to alter the preferred direction of a cell by rotating salient visual cues in the environment (Taube et al., 1990b; McNaughton et al., 1991; Mizumori and Williams, 1993; Goodridge and Taube, 1995; Taube, 1995). This suggests that head-direction cells might rely strongly on vision.

In addition, however, once head-direction cells have established stable directional firing, they can maintain this firing if salient visual landmarks are removed (Taube et al., 1990b), and even in complete darkness (Taube et al., 1988; McNaughton et al. 1991; Mizumori and Williams, 1993). To account for this, it has been proposed that head-direction cells might have the ability to calculate the current directional heading by combining information about the previous head direction and the velocity at which the head is turning (McNaughton et al., 1991). That is, neurons might compute the directional position of the head by integrating the angular motion of the head over time.

This velocity hypothesis is supported by the existence of cells which fire as a function of angular head velocity in PSC (Sharp, in press), and in several anatomically related areas, including visual cortex (Vanni-Mercier and Magnin, 1982) and sensorimotor and posterior parietal areas (McNaughton et al., 1994). Also, some PSC head-direction cells change their firing rate depending on angular head velocity (Taube et al. 1990a).

Here, we report that head-direction cells in ADN shift their direction of firing, depending on the angular velocity of the animal's head. As explained below, this directional shift occurs in a systematic manner, such that ADN cells anticipate the future direction of the animal's head. By contrast, most PSC cells do not shift their directional preference, and thus appear to encode the present direction of the head. Since PSC and ADN are strongly interconnected (van Groen and Wyss, 1990), we hy-

Received Feb. 13, 1995; revised Apr. 14, 1995; accepted May 24, 1995.

We acknowledge the Yale Center for Theoretical and Applied Neuroscience (CTAN) for assistance in preparing the manuscript and illustrations. We thank Steve Fisher, Gretchen Parker, and Kent Fitzgerald for their helpful comments. This work was supported by NSF Grant 9120131 to P.E.S.

Correspondence should be addressed to Hugh T. Blair, Department of Psychology, Yale University, P.O. Box 208205, Yale Station, New Haven, CT 06520-8205.

pothesize that PSC and ADN may form a thalamocortical circuit, which computes the directional position of the rat's head by integrating the angular velocity of the head over time.

Materials and Methods

Experimental subjects

The subjects were 16 female Long-Evans rats, weighing 200–250 gm at shipping. The animals were housed singly upon arrival, and had a 12 hr on (8:00 A.M.–8:00 P.M.)/off, light/dark schedule. Animals were divided into two groups for single-unit neural recording. In 12 of the animals, electrodes were implanted in PSC; in 4 of the animals, electrodes were implanted in ADN. More animals were required in the PSC group, because head-direction cells are more easily isolated in ADN than PSC.

Behavioral apparatus

All recording sessions were conducted in a 50.5 cm high, 74.0 cm diameter cylindrical chamber, like that which has been used in earlier studies of postsubicular head-direction cells (Taube et al., 1990a,b). For most animals in the study, the inner wall of the cylinder was painted with a series of eight alternating black and white vertical stripes. However, due to a methodological change which took place in our laboratory during this experiment, a few of the animals in the PSC group were recorded before the stripe pattern was painted on the wall. Thus, for 7 of the 12 animals in the PSC group, the cylinder wall was painted gray, and was mounted with a single white cue card, occupying 100° of arc, which extended from the floor to the top of the cylinder wall. The black-and-white stripe pattern was used for the remaining five animals in the PSC group, and for all of the animals in the ADN group (no individual animal was exposed to both wall patterns). The difference in the wall's appearance has been shown to have no effect on any aspect of PSC cell firing properties, including those presented in this article (Sharp, unpublished observations), and, so, will not be considered further here. The floor of the cylinder was painted uniformly gray, with a water-resistant paint.

The entire cylinder was surrounded by a uniform, circular black curtain which formed an enclosure 175 cm high and 137 cm in diameter at its widest, and then tapered off above this to a diameter of 57 cm, and a height of 213 cm. Illumination was provided by a single 100 W overhead light (located in an inverted position above the curtain), which spread a diffuse, uniform light over the cylinder floor. Also located above the curtain was an automatic dispenser for the remote-controlled delivery of food pellets. Pellets dispensed in this way dropped to a position near the center of the cylinder floor and scattered to random locations throughout the area of the cylinder. The cylinder was located in a room separate from the recording equipment. A speaker located centrally above the cylinder delivered a constant white noise.

Behavioral training

Prior to training, rats were placed on a food deprivation schedule with which they were reduced to 80% of their ad lib weight through limited daily feeding. They were then trained to search for 20 mg food pellets (BioServe, Frenchtown, NJ) that were thrown into a cylindrical apparatus (identical to the cylindrical chamber later used for recording) at pseudorandom locations, at approximately 15 sec intervals (Muller et al., 1987). A total of six training sessions were given, and during this period rats developed a pattern of nearly constant locomotion that lasted throughout the sessions, and resulted in the rat traversing the entire cylinder floor repeatedly throughout the session.

Electrode implantation

As stated above, 12 rats were prepared for chronic recording of cells in PSC, and 4 rats were prepared for recording in ADN. The recording electrodes and surgical implantation have been described elsewhere (Sharp and Green, 1994). Briefly, after training, two driveable microrecording electrodes (one per hemisphere), consisting of six wires each, were chronically implanted. The six separate wires, cut at an approximately 45° angle, consisted of Formvar-insulated, 25 μm diameter, nichrome wire (California Fine Wire Co., Grover City, CA). The electrodes were placed stereotaxically (at coordinates 6.5 mm posterior and 2.5 mm lateral to Bregma for the PSC placements, and 1.6 mm posterior and 1.8 mm lateral to Bregma for the ADN placements) while the rats were deeply anesthetized with pentobarbital. The electrodes were permanently fixed to the skull with dental acrylic and securing screws. At surgery, the electrode tips were placed below the brain surface (at a depth of 2.0 mm in the PSC group, and 3.5 mm in the ADN group), so that their tips were well above the cells to be recorded, and could be gradually lowered through these layers after recovery.

Unit isolation and data collection

After recovery from surgery, animals were given screening/recording sessions during which the activity from the electrode wires was monitored while the rat performed the pellet-retrieving task in the cylinder. If no single cell activity was present, the electrode bundles were lowered slightly (between 0.022 and 0.044 mm) and the wires were checked again (up to four times of repeated lowering and checking per day). Upon isolation of activity from a single cell(s), a recording session (see below) was initiated. Two wires could be recorded from at the same time, and the signal from each wire was passed first through a field-effect transistor (in source-follower configuration) that was mounted on the pin attached to each electrode wire. This signal then passed through a cable (affixed to the connector on the animal's head) to an amplifier (gain between 5000 and 20,000) and filter (300 Hz, high pass, and 10 kHz, low pass), and then to a computer, for automatic data collection. The software used for data collection and cell discrimination (Brainwave Corporation) collected an epoch of the digitized analog signal for every neural spike event from the amplifier which exceeded a user-set threshold. These events were then separated into bins by a cluster analysis routine, which utilized information from eight different waveform parameters. In this way, it was often possible to collect data from more than one cell simultaneously. Each event, along with a timestamp, and indication of which bin it belonged to, was automatically stored.

The waveforms from any one bin were considered as acceptable for inclusion in the data set if (1) there was judged to be a good signal-to-noise ratio at the time of recording, and the waveforms appeared uniform in shape, and (2) there was a refractory period of 1 to 2 msec between spikes.

Behavioral data collection

The animals' moment-to-moment position in the cylinder was sampled continuously throughout each session. For this, a video camera located above the cylinder monitored the location of two light-emitting diodes attached to the animal's head. One of these lights was toward the front, while the other was toward the back of the animal's head. The video signal was sent to a camera tracking system (Brainwave Corporation) which sampled the location of each of the two lights at a rate of 60 Hz. The lights were spaced sufficiently far apart, so that off-line software could be used to distinguish the front and rear headlights from one another, based on the fact the front headlight leads most of the animal's movements. All session data was timestamped and automatically stored, for use in deriving the following information about the animal's navigational behavior:

Position. The animal's location at each sample time was calculated as the midway point between the front and rear headlights.

Head direction. The animal's momentary head direction was calculated as the angle formed between two lines: the line which passed through the animal's front and rear headlights, and an imaginary line passing through the rear headlight only that was horizontal to the video camera's stationary reference. This yielded a measure of the animal's head direction with respect to the static environmental framework.

Angular head velocity. The momentary angular velocity of the animal's head was calculated as the difference in the angle of head direction between successive 60 Hz time samples.

Recording sessions

To begin each screening/recording session, the rat was carried into the curtained enclosure (surrounding the cylinder) in an enclosed carrying cage, and the animal was held on the experimenter's shoulder while it was attached to the recording cable. The animal was then placed into the cylinder (in the same position each time), and automatic delivery of food pellets was initiated. The signal from each recording wire was screened for single cell activity, and upon isolation of a single cell, a recording session was begun. Throughout each session the animal continuously chased food pellets, and the cell activity, as well as the position of the animal's headlights, was continuously recorded.

In both the PSC and ADN groups, data was collected for a period of approximately 30 min. However, only the first 15 min of the ADN

sessions were included in this study, whereas all 30 min of the PSC sessions were included. There were two reasons for this. First, ADN cells fired about twice as fast as PSC cells, and to balance the power of statistical tests, it was necessary to use shorter sessions for ADN animals, in order to equalize the number of spike events per session in the two groups (see below). Second, some of the ADN animals were exposed to experimental manipulations of the cylindrical chamber after 15 min of recording, in order to collect data for a different study. These manipulations involved rotating the floor and/or wall of the chamber by 90°. In this study, we did not want to include data collected after the manipulation of the cylinder, since such a manipulation could possibly influence the behavior of a cell. However, it should be emphasized that exposure to manipulations in previous recording sessions had no effect on the firing properties of ADN cells examined in this study. That is, the pattern of results we observed for ADN neurons was identical for naive animals and animals that had been exposed to a manipulation in a previous session.

At the end of the session, the animal was returned to its home cage in the enclosed carrying cage. Sessions were conducted on a daily basis for each animal until the electrodes had been lowered to a point at which cellular activity disappeared, indicating that the electrode tips were below the cell layer of interest.

Data presentation and analysis

Although some head-direction cells were recorded during several sessions over consecutive days, only one session's worth of data from each cell was included in the analyses that follow. For those cells which were recorded over multiple sessions, one of the sessions was selected at random for inclusion in the analysis.

Tuning curves. We define a head-direction cell's "tuning curve" as the distribution of its firing rate over the 360° range of possible head directions (see Fig. 1*A,B*). To display a cell's tuning curve, the firing rate of the cell must be computed as a function of the animal's momentary head direction. For this, the 360° range of possible head directions was subdivided into 60 bins, each covering 6° of arc. Every time the animal's headlights were sampled by the video tracking system (at 60 Hz), the momentary head direction was determined (by the method described above) and rounded to the nearest 6° bin. A "visit counter" for that bin was then incremented by one, to indicate a new instance of the animal facing in the direction of that bin. Every time a neural spike occurred during a session, a "spike counter" for the current head-direction bin was incremented by one. At the end of the session, the value of the spike counter was divided by the value of the visit counter for each directional bin, yielding an estimate of the cell's average firing rate for each possible head direction. Taken together, the firing rates for all directions make up the tuning curve.

Mean firing direction (μ). The tuning curve provides the distribution of a head-direction cell's spike frequency over the animal's momentary head direction. We estimated a cell's mean firing direction, which we shall denote as μ, by taking the mean of this distribution.

To compute μ, the animal's momentary head direction was recorded each time a neural spike occurred. At the end of the recording session, all of these recorded head directions were averaged together, yielding the mean direction in which the cell fired. Because head direction was measured on a 0–360° scale, it was necessary to prevent spurious estimates of μ from occurring when a cell's directional peak overlapped the boundary between 0° and 360°. To prevent this, the directional peak was translated before the directional average was taken, so that there was zero overlap between the directional peak and the 0–360° boundary. After the average was taken, the result was then retranslated back to the original angular coordinate system to find the actual value of μ.

Tuning width (ω). The tuning curve of a head-direction cell represents an approximately guassian distribution of spike frequency over head direction, whose peak is centered over the mean firing direction, μ. Thus, the cell fires most rapidly when the rat's head is facing in the direction μ, less rapidly when the head faces directions that are close to μ, and not at all when the head faces directions that are far from μ. The cell's tuning width, ω, reflects the amount of generalization around the mean firing direction, μ.

The simplest way to measure a cell's tuning width, ω, would be to define ω as the standard deviation of the tuning curve, σ. However, σ can be influenced by factors other than the cell's actual tuning width. For example, if the noise baseline differs for two recording sessions, then the session with the lower noise baseline will have a smaller σ value, even if the actual tuning widths of the cells are identical for both sessions. For this reason, we chose an alternative method for measuring ω, which is less susceptible to such errors.

To measure ω, we first found the mean firing direction μ. The maximal firing rate of the tuning curve was then computed as the average firing rate of the cell when the head was facing in the direction μ. This maximal firing rate was then divided by two, yielding the half-maximal firing rate of the cell's tuning curve. We then found the directions on either side of μ at which the cell's average firing rate fell below the half-maximal rate. We denote the half-maximal direction on the left of μ as HL, and the half-maximal direction on the right of μ as HR. The cell's tuning width, ω, was computed as $\omega = HR - HL$, the angular separation between the tuning curve's half-maximal directions on either side of μ.

Analysis of clockwise and counterclockwise head turns. To evaluate the influence of angular head velocity on a cell's firing rate, separate analyses were performed on spikes which occurred during clockwise versus counterclockwise turns of the animal's head. To do this, the angular velocity of the head, as well as the animal's momentary head direction, were recorded each time a neural spike occurred. As explained above (see "Behavioral Data Collection"), the measurements of angular head velocity and head direction were both sampled at a rate of 60 Hz. However, the head velocity and head direction were sampled 180° out of phase with one another, since the angular head velocity was computed as the difference between successive measurements of head direction, and thus represents the average velocity between successive samples. To correct for this phase difference, the animal's head direction was interpolated between successive samples, to yield a new series of head direction measurements that was in phase with the series of angular velocity measurements. Thus, when a spike occurred, the animal's head direction was recorded as the most recently interpolated head direction value, and the angular head velocity was recorded as the most recently derived velocity value.

At the end of the recording session, the head direction measurements were separated into three different turning conditions—clockwise (CLK), counterclockwise (CNT), and still (STILL)—depending upon the angular head velocity during the spike when the head direction was recorded (see Fig. 1*C,D*). Denoting the angular head velocity as v, we adopt the convention that v is positive during clockwise head turns, and v is negative during counterclockwise head turns. The CLK condition was defined as samples for which $v > 90°$/sec, the CNT condition was defined as samples for which $v < -90°$/sec, and the STILL condition was defined as samples for which $|v| < 30°$/sec. If $30 < |v| < 90°$/sec, then the sample was not included in the CLK, CNT, or STILL categories. Therefore, the head had to moving at a speed of at least 90°/sec to be counted as turning.

Statistical comparison of μ^{CLK} and μ^{CNT}. We denote a cell's mean firing direction (as defined above) during clockwise head turns as μ^{CLK}, during counterclockwise head turns as μ^{CNT}, and when the head is not turning as μ^{STILL}. To determine whether a head-direction cell had a different mean firing direction during clockwise versus counterclockwise head turns, a two-tailed t test was performed, comparing the values of μ^{CLK} and μ^{CNT}. Thus, the t test compared the head direction values (current directional heading) for each spike which occurred during clockwise turns, against the head direction values for each spike which occurred during counterclockwise turns. Note that head direction is measured on a 360° scale with degrees increasing left-to-right in the clockwise direction, so that if $\mu^{CLK} < \mu^{CNT}$, then the clockwise mean direction, μ^{CLK}, is to the left of the counterclockwise mean direction, μ^{CNT}. Conversely, if $\mu^{CLK} > \mu^{CNT}$, then μ^{CLK} is to the right of μ^{CNT}.

It should be noted that the degrees of freedom for the t test depended upon the number of spikes in the recording session. Therefore, it was important to try to equalize the number of spike events per session in the PSC and ADN groups. As described below under Results, ADN cells fired about twice as fast as PSC cells. For this reason, although both PSC and ADN cells were recorded for an average of 30 min per session, only the first 15 min of the ADN sessions were included in the analysis, whereas all 30 min were included from PSC cells. Consequently, the power of the t tests was similar in both groups of animals.

Fast and slow head turns. To analyze how the speed of head turns affected the firing rate of head-direction cells, head turns were separated into "fast" and "slow" turns. Fast turns were defined as samples for which the turning speed was greater than 270°/sec, and slow turns were defined as samples for which the turning speed was less than or equal to 270°/sec. If the turning speed was less than 30°/sec, then the head was assumed not to be turning.

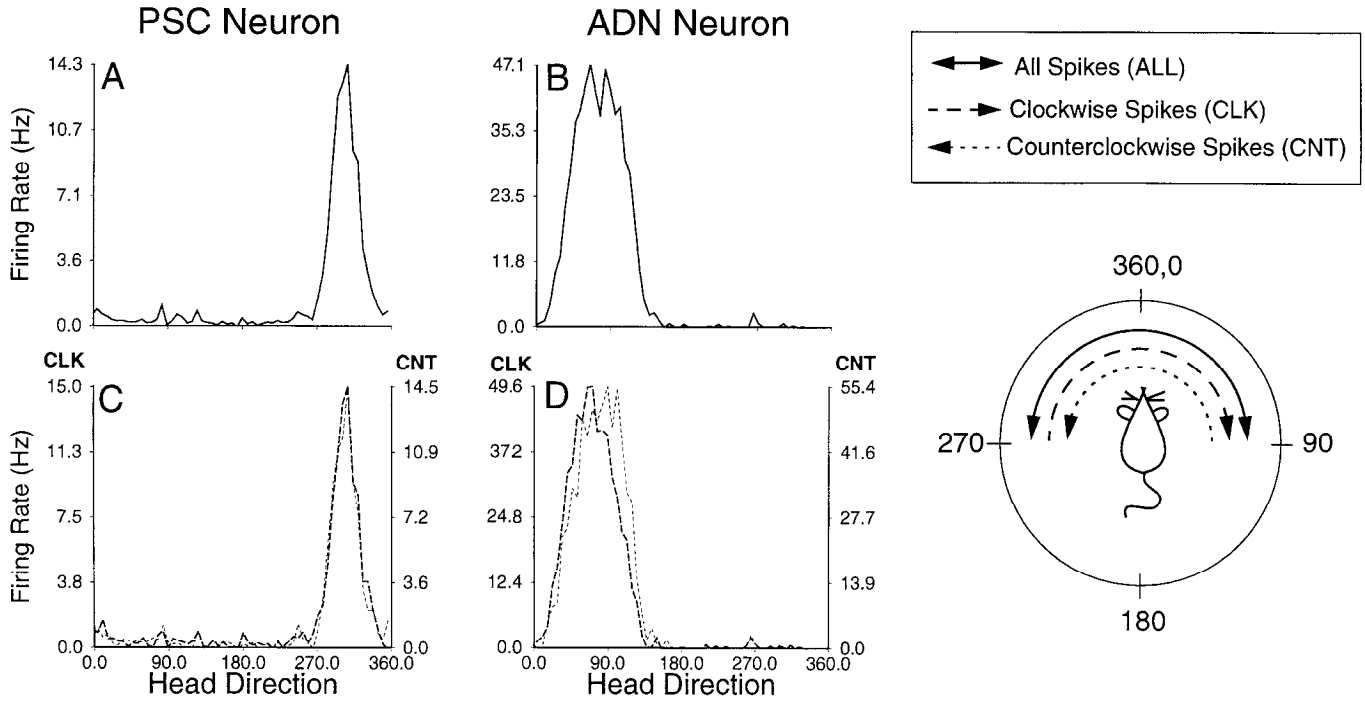

Figure 1. Tuning curves for a typical PSC neuron (*A, C*) and a typical ADN neuron (*B, D*). *A* and *B* show average firing rate as a function of head direction, for all samples taken over the course of the recording session. Both the PSC cell (*A*) and the ADN cell (*B*) show a distinct peak of activity when the animal faces in a specific direction. *C* and *D* show average firing rate as a function of direction broken down into samples which were taken during clockwise (*thick dashed line*) and counterclockwise (*thin dashed line*) turns. The PSC cell maintains the same directional peak regardless of which way the head is turning (*C*). However, for the ADN cell, the directional peak during clockwise head turns is displaced to the left, and the directional peak during counterclockwise head turns is displaced to the right (*D*). Thus, ADN cells appear to shift their optimal firing direction as a function of angular head velocity.

By subdividing head turns according to both turning speed and turning direction, five turning conditions are defined over v, the angular head velocity: (1) fast clockwise turns (CLKfast), for which $v \geq 270°$/sec; (2) slow clockwise turns (CLKslow), for which $30 \leq v < 270°$/sec; (3) fast counterclockwise turns (CNTfast), for which $v \leq -270°$/sec; (4) slow counterclockwise turns (CNTslow), for which $-270 < v \leq -30°$/sec; and (5) no turning at all (STILL), for which $-30 < v < 30$.

Angular separation (δ). In order to quantify the difference between a cell's clockwise mean direction, μ^{CLK}, and its counterclockwise mean direction, μ^{CNT}, the angular separation, δ, between these two values was computed as the difference $\delta = \mu^{CNT} - \mu^{CLK}$. In addition, the angular separation for fast turns was defined as $\delta^{fast} = \mu^{CNTfast} - \mu^{CLKfast}$, and the angular separation for slow turns was defined as $\delta^{slow} = \mu^{CNTslow} - \mu^{CLKslow}$.

Time shift analysis. Each neuron's firing rate was calculated not only as a function of the animal's present head direction, but also as a function of the animal's past and future head directions. The result was a set of time-shifted tuning curves for each cell, which showed the cell's directional tuning for past and future head directions. Time shifts were performed in increments of 16.7 msec, because of the tracking system's 60 Hz sampling rate (see Figs. 6 and 7). Each cell's spike activity was analyzed in relation to the past and future behavior of the animal, exactly as described above for the analysis of present head direction.

Histological examination and reconstruction of cell location

After all recording was completed, animals were placed under deep pentobarbital anesthesia, and a small current (30 μA for five sec) was passed through one wire of each electrode, in order to mark the location of the electrode tips. The animal was then perfused transcardially with a formyl saline solution. The brains were removed and sectioned in the coronal plane into 40 μm slices. The slices were then mounted, and stained with both cresyl violet and Prussian blue. All electrode tracks in the PSC group were found to have passed through the postsubiculum, and all tracks in the ADN group passed through the anterodorsal thalamic region.

Results

Cell sample

In the PSC group, data were collected from 19 head-direction cells in 12 hemispheres of 12 animals. The average firing rate of a PSC head-direction cell, when the rat was facing in the cell's peak firing direction, was 24.3 Hz (±3.7). The average firing rate over all directional samples was 5.7 Hz (±1.3). The average spike width of PSC cells (measured as the interval between the initial departure from and subsequent return to baseline) was 345.0 μsec (±19.0). The average spike amplitude (from peak negativity to peak positivity) was 292.9 μV (±16.8). The average directional tuning width, ω, for PSC neurons was 63.9 (±6.3) degrees.

In the ADN group, data were collected from 21 head-direction cells in six hemispheres of four animals. The average firing rate of an ADN head-direction cell, when the rat was facing in the cell's peak direction, was 66.6 Hz (±14.5). The average firing rate over all directions was 12.3 Hz (±1.0). The average spike width of ADN cells was 241.0 μsec (±9.8), and the average spike amplitude was 237.8 μV (±17.7). The average directional tuning width, ω, for ADN neurons was 69.4 (±3.9) degrees.

In both the PSC and ADN groups, across the cells recorded, the preferred directions of head-direction cells were uniformly distributed over the 360° range of possible directional preferences. That is, no specific direction was favored over any other for being encoded by head-direction cells, a finding which is consistent with previous studies (Taube et al., 1990a; Taube, 1995).

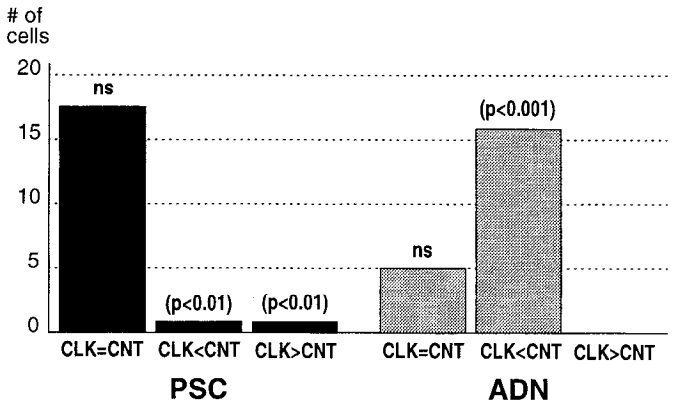

Figure 2. Bar graph showing the number of cells in PSC and ADN that had a significant difference between their clockwise mean firing direction, μ^{CLK}, and their counterclockwise mean firing direction, μ^{CNT}. The label above each bar indicates the minimum effect size of the difference between μ^{CLK} and μ^{CNT} for any cell included under that bar. The graph shows that for all but two of the PSC neurons, μ^{CLK} was not significantly different from μ^{CNT}. By contrast, for all but five of the ADN cells, $\mu^{CLK} < \mu^{CNT}$. As explained in the text, this suggests that PSC cells encode the present head direction, while ADN cell encode the future head direction.

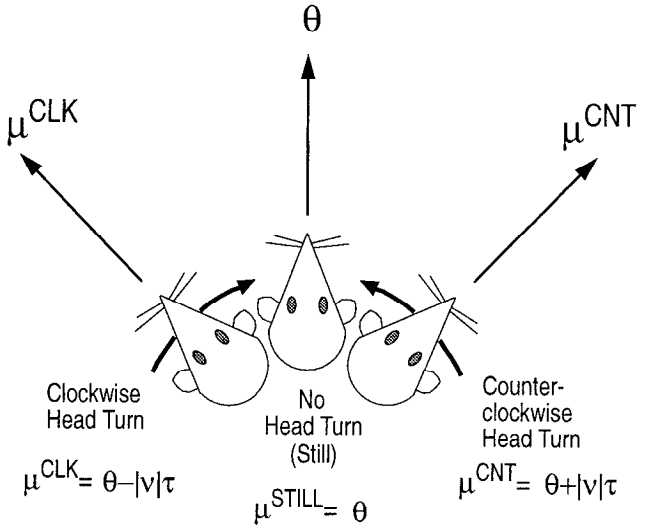

Figure 3. Illustration of how an anticipatory head-direction cell must behave, in order to predict that the rat's head will face a specific direction θ after a specific time delay τ (see Equations 1 and 2). The figure assumes that μ is measured in degrees, with degrees increasing in the clockwise direction. If the rat is turning clockwise at positive velocity v to approach the direction θ from the left, then the cell must fire to the left of θ, in the direction $\mu = \theta - |v|\tau$. If the rat is turning counterclockwise at negative velocity v to approach θ from the right, then the cell must fire to the right of θ, in the direction $\mu = \theta + |v|\tau$. If the animal is not turning its head, then the cell must fire only when the animal is facing in the direction $\mu = \tau$ (see text).

Tuning curves

Figure 1 illustrates tuning curves for two typical examples of head-direction cells, one recorded from PSC, and the other recorded from ADN. In Figure 1, *A* and *B*, the spike frequency of each neuron is plotted as a function of the animal's momentary head direction. Like all of the head-direction cells we recorded, both of the cells in Figure 1 exhibit a distinct peak in their tuning curve, centered over the preferred direction of the cell. To examine the influence of angular head velocity upon the cells' firing rates, the tuning curve of each cell was plotted separately for spikes which occurred during clockwise versus counterclockwise turns of the animal's head (see Materials and Methods). This yielded two separate tuning curves (one for each turning condition), as shown in Figure 1, *C* and *D*. Most head-direction cells in PSC fired in the same mean direction, no matter which way the head was turning (Fig. 1*C*). By contrast, most head-direction cells in ADN shifted their mean directional preference to the left during clockwise turns, and to the right during counterclockwise turns (Fig. 1*D*).

Because the distribution of spike frequency over head direction was approximately guassian, it was possible to perform a *t* test on the data from each cell, to determine which cells had a significantly different mean firing direction during clockwise versus counterclockwise head turns. As described in Materials and Methods, the mean firing direction of a cell, which we shall denote as μ, was computed by recording the animal's head direction each time a spike occurred, and then averaging these recorded head directions together over an entire recording session. The mean firing directions for clockwise and counterclockwise turns, μ^{CLK} and μ^{CNT}, were calculated by separately averaging head directions for spikes which occurred during each turning condition. For each cell, the distributions represented by μ^{CLK} and μ^{CNT} were compared, using a two-tailed *t* test. Because ADN cells fired much faster than PSC cells, adjustments were made to the length of recording sessions, to insure that the power of the *t* tests were similar in the PSC and ADN groups (see Materials and Methods).

Figure 2 summarizes the results of the *t* test comparisons. Of the 19 cells recorded in PSC, only two cells fired in a significantly different direction during clockwise versus counterclockwise turns. For one of these two cells $\mu^{CLK} < \mu^{CNT}$ ($p < 0.01$), and for the other cell $\mu^{CLK} > \mu^{CNT}$ ($p < 0.01$). Of the 21 head-direction cells recorded in ADN, 16 cells showed a significant difference between their clockwise and counterclockwise directional means (it should be noted that the remaining five cells were evenly distributed across experimental animals, such that in each ADN animal, there was at least one cell for which μ^{CLK} and μ^{CNT} were not significantly different). For every one of these 16 cells, $\mu^{CLK} < \mu^{CNT}$ (minimum effect size, $p < 0.001$). That is, for all 16 of the ADN cells with unequal mean direction values, the mean firing direction was displaced to the left during clockwise turns, and to the right during counterclockwise turns, and never vice versa. For 14 of these 16 cells, the mean firing direction when the animal was not turning, μ^{STILL}, was in between the clockwise and counterclockwise directional means. Therefore, for 14 out of 21 ADN cells, it was found that $\mu^{CLK} < \mu^{STILL} < \mu^{CNT}$.

Anticipating the future head direction

These observations suggest that PSC cells fire when the head is presently facing a specific direction, whereas ADN cells fire when the head will be facing a specific direction in the near future. That is, it appears that PSC cells may encode the present direction of the rat's head, whereas ADN cells may anticipate the future direction of the rat's head. To see why this might be so, consider a cell that predicts the rat's head will be facing a certain direction, θ, in the near future (see Fig. 3). There are three possible turning conditions. First, if the head is turning clockwise and approaching the direction θ, then the anticipatory cell must fire to the left of θ, since being to the left of θ and

turning clockwise predicts arrival at θ in the near future. Second, if the animal is turning counterclockwise to approach the direction θ, then the anticipatory cell must begin firing while the head is to the right of θ. Third, if the animal is not turning, then the future and present head directions are the same, so an anticipatory cell should behave identically to a cell which encodes the present head direction, and fire when the animal is facing in the direction θ.

In summary, if a cell anticipates the future head direction, then it must shift its mean firing direction to the left during clockwise turns, and to the right during counterclockwise turns. If a cell encodes the present head direction, then it should have the same mean firing direction, regardless of which way the head is turning. Note that if a cell encodes the past head direction, then it would have to shift its mean firing direction to the right during clockwise turns, and to the left during counterclockwise turns.

Based on these relations, a head-direction cell's mean firing direction can be estimated, to a first order of approximation, by the equation

$$\mu(v) = \theta - v\tau, \tag{1}$$

where μ is the cell's mean direction of firing (as defined above), θ is the "anticipated direction" that the cell encodes, v is the momentary angular velocity of the head (which is positive for clockwise head turns, and negative for counterclockwise head turns), and τ is the time delay by which the cell anticipates that the head will face the direction θ. According to Equation 1, there are three possible behavior patterns for head-direction cells, depending on whether the τ parameter is positive, negative, or zero.

If $\tau = 0$, Equation 1 is reduced to $\mu = \theta$. This constitutes a special case, in which the neuron encodes the present head direction. In this special case, the neuron fires maximally when the head is facing θ, regardless of the angular velocity of the head. This is how most PSC cells behaved (see Fig. 1), suggesting that they encoded the present head direction.

If $\tau > 0$, then the neuron encodes the future head direction, and there are three turning conditions to consider. First, if the head is turning clockwise and approaching the direction θ, then $v > 0$, and thus $\mu^{CLK} < \theta$. Second, if the head is turning counterclockwise, then $v < 0$, and thus $\mu^{CNT} > \theta$. Third, if the head is not turning, then $v = 0$, and thus $\mu^{STILL} = \theta$. In summary, Equation 1 predicts the relation $\mu^{CLK} < \mu^{STILL} < \mu^{CNT}$ for anticipatory head-direction cells. This is how most ADN cells behaved (see Fig. 1), suggesting that they anticipated the future head direction.

If $\tau < 0$, then the neuron encodes the past head-direction, and it follows that $\mu^{CLK} < \mu^{STILL} < \mu^{CNT}$. None of the head direction cells we recorded behaved in this manner.

Equation 1 provides a simple formula for predicting how head-direction cells should behave, if they anticipate the rat's head direction by a specific time delay, τ. In the analyses that follow, we shall demonstrate that Equation 1 does indeed provide a good description of head-direction cell behavior in ADN. However, it should be noted that Equation 1 considers only the angular head velocity, and ignores other factors, such as angular head acceleration. Thus, if ADN cells anticipate the future head-direction, as we have proposed, then Equation 1 may be less accurate at predicting the behavior of these cells during periods of significant angular head acceleration. Our purpose here is to establish that ADN neurons shift their directional preference, in a manner which is consistent with the notion that they anticipate the future head direction. For simplicity, our analyses shall examine cell activity only in relation to angular head velocity, ignoring the possible contributions of angular head acceleration. This issue is discussed further in the discussion section.

Magnitude of directional shift

If we define the angular separation, δ, between a neuron's clockwise and counterclockwise mean firing direction as the difference

$$\delta = \mu^{CNT} - \mu^{CLK} = 2\,|v|\tau, \tag{2}$$

then we should find that $\delta = 0$ for neurons encoding the present head direction (because $\tau = 0$), whereas δ is proportional to v for neurons encoding the future head direction (because $\tau > 0$). Figure 2 indicates that $\delta = 0$ for most head-direction cells in PSC, and $\delta > 0$ for most head-direction cells in ADN. This observation is consistent with the hypothesis that PSC cells encode the present direction of the head, whereas ADN cells encode the future direction of the head. However, if ADN cells encode the future head direction by some fixed time delay τ, then it should be possible to show that δ is not only positive for ADN cells, but also proportional to the angular speed of the head, as expressed in Equation 2. This is because during relatively fast turns, the cell must signal arrival at θ at a further distance away from θ than for slower turns, as formalized by Equation 1. Hence, the value of δ should increase in proportion with the angular speed of the animal's head.

To test this prediction, head turns made by the animal were subdivided according to their speed into two categories: "fast" and "slow" turns (see Materials and Methods). In the ADN animals, the average speed of fast turns was 455°/sec, and of slow turns was 165°/sec. In the PSC animals, the average speed of fast turns was 436°/sec, and of slow turns was 163°/sec.

Two angular separation values were computed for each head direction cell: δ^{fast} and δ^{slow}, with $\delta^{fast} = \mu^{CNTfast} - \mu^{CLKfast}$ and $\delta^{slow} = \mu^{CNTslow} - \mu^{CLKslow}$ (see Materials and Methods). The average angular separation values for ADN cells were $\delta^{fast} = 9.79°$, and $\delta^{slow} = 4.03°$ (Fig. 4). The average values for PSC cells were $\delta^{fast} = 0.72°$, and $\delta^{slow} = 1.50°$ (Fig. 4). A 2×2 ANOVA of angular separation versus turning speed revealed a significant main effect of brain region ($df = 1$, $F = 14.56$, $p < 0.0005$), no main effect of turning speed ($df = 1$, $F = 3.06$, $p > 0.05$), and a significant interaction between brain region and turning speed ($df = 1$, $F = 4.53$, $p < 0.05$). Thus, it appears that ADN cells altered their mean firing direction μ in proportion with angular head velocity, but PSC cells did not. This is what would be expected if PSC cells encode the present head direction, and ADN cells encode the future head direction, θ.

Prediction time delay

We have demonstrated that ADN neurons systematically shift their mean firing direction as a function of angular head velocity, in a manner that suggests these cells anticipate the future head direction. We now turn to the question of how far into the future these cells might anticipate the rat's head direction.

If a neuron's firing predicts the rat's head direction by a specific time delay, τ, then it should be expected that the neuron will have its best tuning function at a time delay equal to τ. The "best" tuning function may be defined as that for which the cell's tuning width, ω, is narrowest. Thus, by plotting a cell's firing rate as a function of past, present, and future head direc-

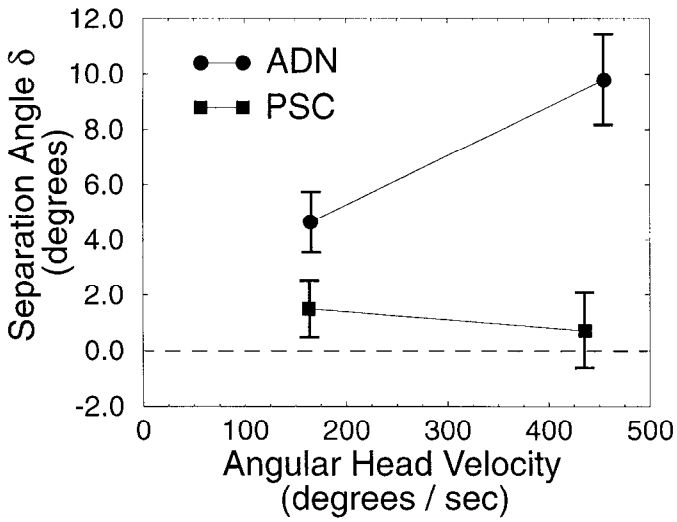

Figure 4. The average angular separation values between clockwise and counterclockwise turns, δ^{FAST} and δ^{SLOW}, for head-direction cells recorded in PSC (N = 19) and ADN (N = 21). A 2×2 ANOVA revealed that the separation angle increased as a function of angular head velocity for ADN cells, but not for PSC cells (see text). This supports the hypothesis that PSC cells encode the present direction of the head, whereas ADN cells encode the future direction of the head.

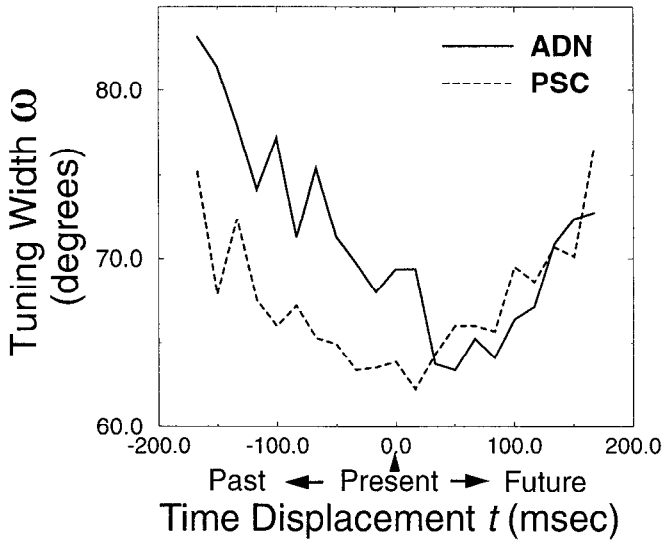

Figure 5. Tuning curves were computed at different time intervals, by pairing spike activity with the rat's head direction across a range of time displacements. The average directional tuning width, ω, is plotted as a function of time displacement, t, for head direction cells in PSC and ADN. From the graph, it is clear that PSC cells have their minimum tuning function at a time displacement of about 0 msec. By contrast, ADN cells have their narrowest tuning width at a positive time displacement of about 40 msec.

tions (see Materials and Methods), and examining the tuning curve at each time delay, it should be possible to estimate the value of τ as the time delay for which the tuning function is narrowest.

Figure 5 shows a graph of average tuning width, θ, as a function of time delay, τ, for cells in PSC and ADN. Note that the minimum tuning width for PSC cells occurs at a time displacement of approximately $\tau = 0$, suggesting that PSC cells encoded the present direction of the head. By contrast, the minimum tuning width for ADN cells occurs at a positive time displacement of about 40 msec, suggesting that ADN cells anticipated the future direction of the head, perhaps by as much as 40 msec. However, it is difficult to obtain a precise estimate of τ from the data in Figure 5.

To obtain a more precise estimate, a second analysis was performed. As in Figure 5, we examined firing rate of each neuron as a function of the animal's past, present, and future head directions, and computed tuning curves at each time displacement. We shall denote the time displacement between firing rate and head direction as t. Note that if a neuron anticipates the future head direction by a time delay of τ, then when t is exactly equal to τ, the time-shifted tuning curve of the anticipatory cell should no longer be affected by angular head velocity. That is, it should be true that $\delta = 0$ at a time displacement of $t = \tau$. We have already shown that for PSC cells, $\delta = 0$ at a time displacement of $t = 0$ (see Figs. 2 and 4), which is consistent with our suggestion that PSC cells encode the present head direction. If it is true, as we have suggested, that ADN cells encode the future direction of the head by a fixed time delay, τ, then it should be possible to estimate τ as the value of t for which $\delta = 0$.

When a cell's firing rate is calculated as a function of future or past head direction, Equation 1 becomes

$$\mu(t) = \theta + v(t - \tau), \quad (3)$$

where t denotes the time displacement between firing rate and head direction. As in Figure 5, we adopt the convention that t is positive for future head directions, and t is negative for past head directions. It is clear that when $t = 0$, Equation 3 is identical to Equation 1, and when $t = \tau$, Equation 3 is reduced to $\mu - \theta$. Therefore, for head directions which occur at precisely τ msec in the future, an anticipatory cell's mean firing direction μ should always be equal to θ, regardless of the angular head velocity.

To obtain an accurate estimate of τ, each neuron's tuning curve was calculated independently at different time displacements, by varying t over a range of −83.5 to +83.5 in increments of 16.7 msec (see Materials and Methods). This procedure resulted in two time series of δ values for each neuron: a δ^{fast} time series, and a δ^{slow} time series. The values of δ^{fast} and δ^{slow} were averaged within each group of animals at each time displacement, yielding an averaged δ^{fast} time series and an averaged δ^{slow} time series for both the PSC and ADN cells. The results of this analysis are illustrated in Figures 6 and 7.

In Figure 6, the time series of δ^{fast} and δ^{slow} for the PSC and ADN groups are shown beside a series averaged tuning curves. The averaged tuning curves were generated by plotting a tuning curve for each cell under each turning condition, and normalizing the firing rate of each curve with respect to its maximum value. The normalized tuning curves for each turning condition were then centered on top of each other, by aligning them with respect to their directional means, and averaged together over all cells in each group. The separation between these averaged tuning curves corresponds well with the average separation angle, δ. It can be seen that in the PSC group, both δ^{fast} and δ^{slow} become zero at a time displacement of about $t = 0$ msec, whereas in the ADN group, both δ^{fast} and δ^{slow} become zero at a time displacement of between t = 33.4 and t = 50.1 msec. This suggests that τ is approximately zero for PSC cells, and τ is a larger positive value for ADN cells.

To obtain more accurate estimates of τ, lines were fitted to the sequence of points given by δ^{fast} and δ^{slow} over successive

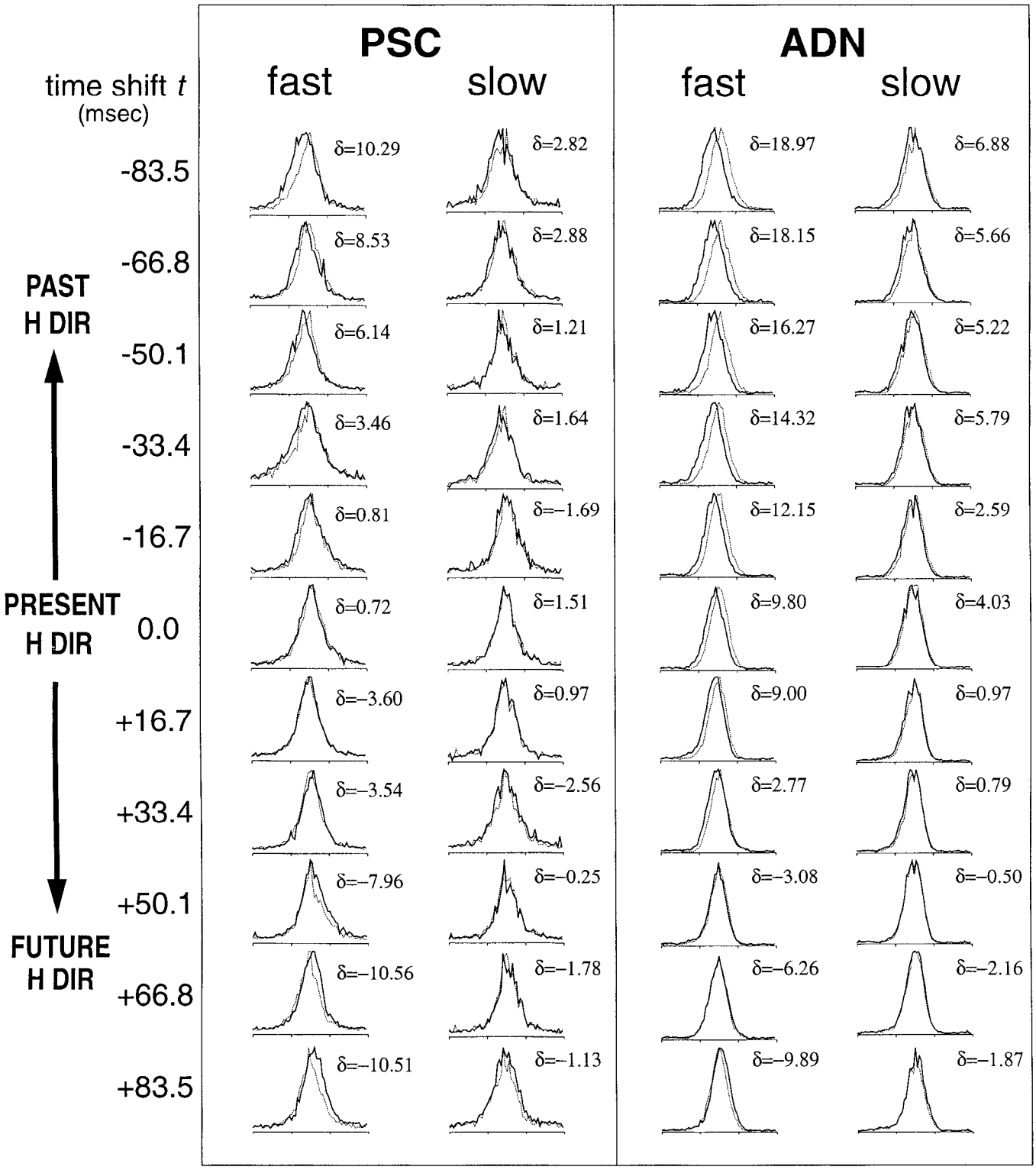

Figure 6. Averaged tuning curves with corresponding δ values, for fast and slow head turns in PSC and ADN cells. *Bold lines* indicate spike activity during clockwise turns, and *thin lines* indicate spike activity during counterclockwise turns. The angular separation, δ, between μ^{CLK} and μ^{CNT} becomes zero at a time displacement of approximately $t = 0$ for PSC cells. This is consistent with the hypothesis that PSC cells encode the present head direction. By contrast, δ becomes zero at a time displacement in between 33.4 and 50.1 msec for ADN cells, consistent with the hypothesis that ADN encode the future head direction.

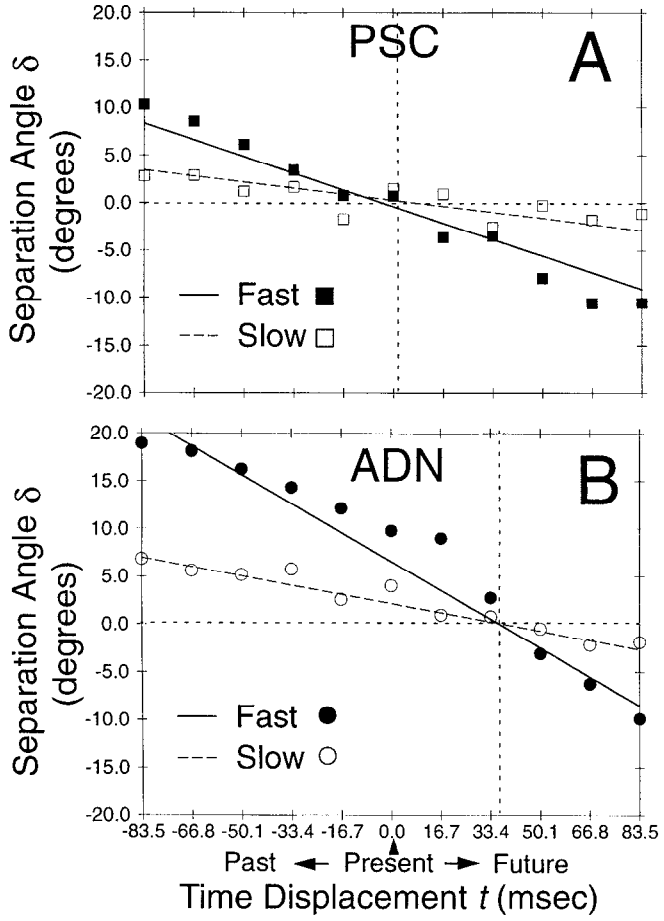

Figure 7. Estimated values of τ for fast and slow turning conditions, derived by fitting lines to each sequence of δ values from Figure 6. *A*, For PSC cells, δ^{FAST} and δ^{SLOW} both intercept zero at a time displacement of approximately $t = 0$ msec, indicating that PSC cells encode the present head direction. *B*, For ADN cells, δ^{fast} and δ^{slow} both intercept zero at a time displacement of about +37 msec, indicating that ADN cells encoded the future direction of the head by about 37 msec.

time intervals, and τ was estimated as the point where these lines crossed the horizontal axis at $\delta = 0$ (Fig. 7). In the PSC group, δ^{fast} and δ^{slow} crossed zero at time intervals of $t = -3.61$ msec and $t = +7.63$ msec, respectively, giving a mean estimate of $\tau = 2.01$ msec. In the ADN group, δ^{fast} and δ^{slow} crossed zero at $t = +36.33$ msec and $t = +37.42$ msec, respectively, giving a mean estimate of $\tau = 36.875$.

In summary, Figures 6 and 7 show that the estimated value of t was near zero for PSC cells, suggesting that they encoded the present head direction. By contrast, the estimated value of t was much larger for ADN cells, suggesting that they encoded the future direction of the head by an average of about 37 msec.

Velocity-dependent changes in firing rate

Our data show that ADN cells shift their mean firing direction as a function of angular head velocity, whereas PSC cells maintain the same firing direction, no matter which way the head is turning. We therefore investigated whether the observed change in firing direction for ADN cells is accompanied by a corresponding change in firing rate.

Figure 8 shows the average firing rate of head-direction cells in PSC and ADN, as a function of angular head velocity. The graph was created by plotting the average firing rate of the cells

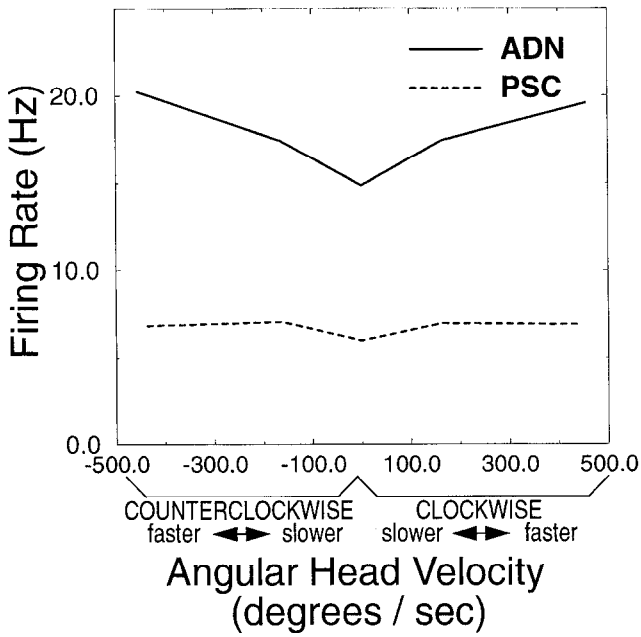

Figure 8. Average firing rate, in Hz, as a function of angular head velocity, in degrees per second. ADN cells fire at a higher rate during fast head turns, and a slower rate during slow head turns. PSC cells have about the same firing rate, no matter how fast the head is turning.

for the fast, slow, and still turning conditions. The graph shows that ADN cells increased their average firing rate as a function of angular head velocity, whereas as PSC cells had the same average firing rate, no matter how fast the head was turning. The functional implications of this result are discussed below.

Discussion

We have shown that head-direction cells in PSC do not change their mean firing direction as a function of angular head velocity, whereas head-direction cells in ADN shift their mean firing direction systematically as a function of angular head velocity. For ADN cells, the mean firing direction during clockwise turns is always shifted to the left, and the mean firing direction during counterclockwise turns is always shifted to the right. The angular separation, δ, between an ADN cell's clockwise and counterclockwise mean firing directions, is greater for fast turning speeds than for slow turning speeds (Fig. 4). These observations suggest that ADN cells might predict the future direction of the rat's head. Time-shift analysis indicates that the best (narrowest) tuning function for ADN cells occurs when spike activity is correlated with the future head direction, whereas the best tuning function for PSC cells is obtained in relation to the present head direction. On average, the firing of ADN cells anticipates the future head direction by about 37 msec (Fig. 7). These results indicate that PSC cells might encode the present direction of the animal's head, whereas ADN cells may anticipate the future direction of the head.

Functional and anatomical considerations

Why should it be the case that neurons in one brain area encode the present head direction, while neurons in another area anticipate the future head direction? It has been suggested that head-direction cells might rely on a "dead-reckoning" process to maintain an accurate signal of directional heading (McNaughton et al., 1991). This dead-reckoning hypothesis proposes that head-

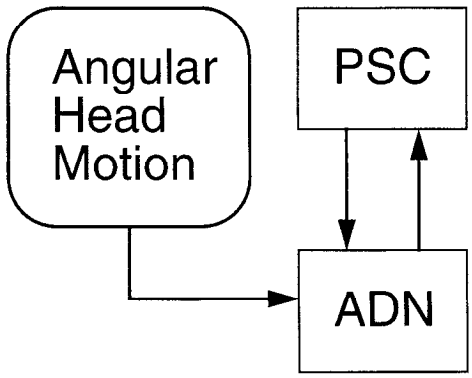

Figure 9. Connections of PSC and ADN. ADN cells, which anticipate the future head direction, send output to PSC cells, which encode the present head direction, thus providing PSC cells with information for updating their representation of the current head direction. In turn, ADN cells receive the signal of present head direction from PSC cells, and combine this signal with information about angular head motion, to anticipate the future head direction.

direction cells might track the direction of the head, by integrating angular head movements over time. Cells that predict the future head direction, by shifting their mean firing direction as a function of angular velocity, might constitute an important functional component of a circuit for dead-reckoning.

PSC and ADN are reciprocally connected with one another (van Groen and Wyss, 1990), and may form a basic circuit for dead-reckoning (Fig. 9). In this circuit, ADN cells that predict the future head direction might project to PSC cells that encode the present head direction, thereby providing PSC cells with "advance notice" about when to update their representation of the present head direction. Likewise, to predict the future head direction, ADN cells might rely upon input from PSC cells that encode the present head direction, combined with information about angular head motion. In addition to its input from PSC, ADN also receives input from retrosplenial cortex (Seki and Zyo, 1984). Cells that fire in relation to the angular head velocity are found in both PSC (Sharp, in press) and retrosplenial cortex (McNaughton et al., 1994). Summarizing, ADN neurons might combine two kinds of information to predict the future head direction: information about the present head-direction, and information about the angular movement of the head. We propose that PSC and ADN might form a thalamocortical circuit, which computes the directional position of the head by integrating angular head motion over time.

Here, we have analyzed the behavior of head-direction cells in ADN, and we have discovered a velocity-dependent shift in the ADN cells' mean firing direction. Our analyses revealed that the properties of this shift are consistent with a first-order prediction of the future head direction, based on angular head velocity, as specified by Equation 1. These results provide good preliminary evidence that ADN cells might encode the future direction of the rat's head. Of course, an accurate dead-reckoning circuit would have to predict the future head direction more precisely than Equation 1, based on angular head acceleration as well as the angular head velocity. In addition, the head-direction system might do more than passively monitor the position and movement of the head. The system might also receive direct input from motor areas, which command the movement of the head, and thus be able to utilize information about impending head movements that have not yet occurred.

It is interesting that ADN cells not only changed their mean firing direction in proportion to angular head velocity, but also increased their firing rate (Fig. 8). As mentioned (see Fig. 9), ADN cells might receive information from cells that fire in proportion to the angular movement of the head. Activation of these inputs during head turns could account for the higher firing rate of ADN cells when the head is turning quickly. Alternatively, ADN cells might be responsive to the derivative of PSC cell activity. When the head is turning quickly, a PSC cell must switch rapidly from an inactive state to an active state, as the head suddenly faces the cell's preferred direction. By contrast, when the head is turning slowly, the firing rate of a PSC cell will ramp up more gradually, as the animal approaches the preferred firing direction of the cell. This difference in the derivative of PSC cell activity might be responsible for the higher firing rate of ADN cells during rapid head turns.

Anticipatory time delay

We have estimated that the firing of ADN cells anticipates the future head direction by an average time delay of about 37 msec. To put this number into perspective, recall that the average speed of "fast" turns was about 450°/sec, and the average speed of "slow" turns was about 160°/sec. If an ADN cell predicts the head will be facing a specific direction, θ, in 37 msec, then during fast turns, the cell must shift its mean firing direction by about 16.7° in order to correctly anticipate arrival at θ. By comparison, during slow turns, the cell must shift its mean firing direction by about 5.9°.

Why should cells in ADN anticipate the future head direction by a delay of 37 msec? One possibility is that, as discussed above, ADN cells are responsible for informing PSC cells to update their representation of the current head direction. If this were true, ADN cells would need to anticipate the future head direction by exactly the amount of time that it takes the neural signal to travel from ADN to PSC. However, given that ADN neurons project directly to PSC neurons (van Groen and Wyss, 1990), the transmission delay between ADN and PSC should be much less than 37 msec. An alternative possibility is that each head-direction cell in ADN has its own characteristic value of τ, and thus, each ADN cell specializes in predicting the future head direction by a specific time delay. If this were the case, then 37 msec would represent the average anticipatory time delay for ADN cells, but some cells would consistently anticipate the future head direction by less than 37 msec, and some cells would consistently anticipate by more than 37 msec. A head-direction cell in PSC, which fires when the head is presently facing a specific direction, θ, might receive input from many different cells in ADN, each of which predicts arrival at θ by a different time delay. The PSC neuron might require sequential activation of its inputs from many of these ADN cells, in order to begin firing. This would provide a "safety mechanism," whereby PSC cells would only fire to indicate the current head direction after receiving input from many different ADN cells, which predict arrival at θ on many different time scales. The low average firing rate of PSC cells supports this notion, since it implies that PSC cells may be difficult to excite.

Summary

In conclusion, we have shown that head-direction cells in PSC appear to signal the present direction of the rat's head, and head-direction cells in ADN appear to anticipate the future direction of the rat's head. We have proposed that PSC and ADN are

reciprocally connected to form a thalamocortical circuit, which computes the directional position of the rat's head by utilizing information about angular head movements. If further experiments support this hypothesis, then the rat head-direction system may provide a good model for investigating the structure and function of thalamocortical circuitry.

References

Chen LL, McNaughton BL, Barnes CA, Ortiz ER (1990) Head direction and behavioral correlates of posterior cingulate and medial prestriate cortex neurons in freely moving rats. Soc Neurosci Abstr 16: 441.

Goodridge JP, Taube JS (1995) Preferential use of the landmark navigational system by head-direction cells in rats. Behav Neurosci 109: 49–61.

McNaughton BL, Chen LL, Markus EJ (1991) "Dead reckoning," landmark learning, and the sense of direction: a neurophysiological and computational hypothesis. J Cognit Neurosci 3:190–201.

McNaughton BL, Mizumori SYJ, Barnes CA, Leonard BJ, Marquis M, Green EJ (1994) Cortical representation of motion during unrestrained spatial navigation in the rat. Cereb Cortex 4:27–39.

Mizumori SJY, Williams JD (1993) Directionally selective mnemonic properties of neurons in the lateral dorsal nucleus of the thalamus of rats. J Neurosci 13:4015–4028.

Muller RU, Kubie JL, Ranck JB Jr (1987) Spatial firing patterns of hippocampal complex-spike cells in a fixed environment. J Neurosci 7:1935–1950.

Ranck JB Jr (1984) Head-direction cells in the deep cell layers of dorsal presubiculum in freely moving rats. Soc Neurosci Abstr 10: 599.

Seki M, Zyo K (1984) Anterior thalamic afferents from the mamillary body and the limbic cortex in the rat. J Comp Neurol 229:242–256.

Sharp PE (in press) Multiple spatial/behavioral correlates for cells in the rat postsubiculum: multiple regression analysis and comparison to other hippocampal areas. Cereb Cortex, in press.

Sharp PE, Green C (1994) Spatial correlates of firing patterns of single cells in the subiculum of the freely moving rat. J Neurosci 14:2339–2356.

Taube JS (1995) Head direction cells recorded in the anterior thalamic nuclei of freely moving rats. J Neurosci 15:70–86.

Taube JS, Muller RU, Ranck JB Jr (1988) Effects of environmental manipulations on the discharge of head-direction cells in the postsubiculum. Soc Neurosci Abstr 14:126.

Taube JS, Muller RU, Ranck JB Jr (1990a) Head-direction cells recorded from the postsubiculum in freely moving rats. I. Description and quantitative analysis. J Neurosci 10:420–435.

Taube JS, Muller RU, Ranck JB Jr (1990b) Head-direction cells recorded from the postsubiculum in freely moving rats. II. Effects of environmental manipulations. J Neurosci 10:436–447.

van Groen T, Wyss MJ (1990) The postsubicular cortex in rat: characterization of the fourth region of the subicular cortex and its connections. Brain Res 529:165–177.

Vanni-Mercier G, Magnin M (1982) Single neuron activity related to natural vestibular stimulation in the cat's visual cortex. Exp Brain Res 45:451–455.

Wiener SI (1993) Spatial and behavioral correlates of striatal neurons in rats performing a self-initiated navigational task. J Neurosci 13: 3802–3817.